MDPI

Climatic Effects on Position and Dynamics of Upper Open Forest Boundary in Altay and Western Sayan in the Last 60 Years

Pavel A. Moiseev and Nail' F. Nizametdinov *

Institute of Plant and Animal Ecology, Ural Branch, Russian Academy of Sciences, 620144 Yekaterinburg, Russia;
moiseev@ipae.uran.ru
* Correspondence: niznail@yandex.ru; Tel.: +7-9221-600-260

Abstract: The upper treeline ecotone is a global and typically climate-dependent phenomenon. Its elevation is usually coupled with the thermal limitations of tree growth. The air temperature rise connected with global warming is assumed as the main cause of treeline upslope shifts in the last century. It has been found that the treeline elevation also correlates with the distance from the coastline and the aridity or continentality of the climate or the mass elevation effect. However, previous and contemporary publications have not explained how the upper treeline position directly couples with climate parameters. Often, this has been restricted by a lack of climate measurements and spatial data. In our study, we obtained data from 339 regional weather stations for 1964–1974 and interpolated them to Altay and Western Sayan using regional DEMs and a specially developed regression model. Moreover, we semiautomatically identified the elevational position of the upper open forest boundary (OFB) (crown closure > 10%) on the slopes of 30 mountains in Altay and Western Sayan in 1960 and 2020. We took into account the slope aspect and edaphic constraints. The obtained data allowed us to undertake a regression analysis of the dependence of the OFB elevation on climatic parameters. As a result, we found that, in the 1960s, at OFB elevations rising from the outer to the inner parts of the study area to approximately 500–700 m, the summer air temperature and precipitation linearly decreased, but the summer sunshine duration increased. In the multiple regression analysis, including the climatic parameters as independent variables and the OFB elevation as a dependent variable, significant relations were found only for the combination of air temperature and sunshine duration. We assume that the OFB elevation is determined not only by the air temperature but also by the direct solar irradiation level, changing with latitude and cloudiness. We also found that the ratio between the OFB elevation on the northern and southern slopes varied with respect to latitude. The spatial analysis of OFB shifts in 1960–2020 revealed significant differences in its value in the central (80–90 m) and outer parts of the study area (110–130 m). We suppose that the OFB advance over the past 60 years has local specificity associated with the peculiarities of the climatic changes (summer temperature rise, precipitation decrease, and sunshine duration increase) in different parts of Altay and Western Sayan. Our results highlight the need to clearly determine climatic parameters when forecasting woody vegetation reactions to future climate changes.

Keywords: upper open forest boundary; climate parameters; edaphic constrains; mass elevation effect; climate change; elevational shift; regression analysis; kriging; Altay; Western Sayan

1. Introduction

In recent decades, numerous publications have been devoted to climate changes' effects on ecosystems. This is related to the need for the modeling of processes in the biosphere and the estimation of the consequences of climate changes for the Earth's ecosystems. According to the Intergovernmental Panel on Climate Change, for the period from 1880 to 2020, the average Earth surface temperature increased by 0.85 °C. It is likely that the doubling of the CO_2 concentration will cause an additional increase in the global temperature by 1–3.5 °C. The most significant changes will take place at high latitudes

and elevations [1]. The structures of plant communities will also change with shifts in temperature and precipitation. In previous publications, a decrease in moisture supply and increase in air temperature in the coming decades were forecasted [2]. Some works have noted insignificant increasing precipitation [3]. The cycle of carbon will be altered and its sequestration will be increased. Earlier observations have shown that plant communities are more sensitive to environmental variations in transition zones, where the thermal and edaphic conditions change drastically in comparably short distances [4,5]. The upper treeline ecotone is an example of such a natural phenomenon [6–8].

Upright-stemmed trees are typically growth-limited due to low summer temperatures at their upper range edges because they are strongly dependent on the ambient air temperature due to the relatively large size of their crowns [9]. Plants with lower stature (shrubs, dwarf scrubs, and grasses) are able to grow at much higher elevations in conditions with a much lower air temperature. The winter temperature plays a minor role in the existence of trees at their upper limits [5,10]. To establish the temperature conditions at the upper treeline, the isotherm of the warmest month at 10 °C is commonly utilized [11]. Previous research revealed that the lowest average monthly air temperature during the growth period equal to 5 °C is a suitable tool to describe the temperature environment at the upper forest line. Paulsen and Körner developed a climate-based model for treeline prediction by defining the growing season as days with a mean temperature above 0.9 °C and with a mean temperature of more than 6.4 °C during that time. They stated that the minimum duration of the growing period for the upper treeline in a global context should not be less than 94 days. Results from studies of the treeline elevation in different parts of the world showed a decrease in this indicator towards high latitudes [8]. High variability (up to 1000 m) in the treeline elevation can also be seen at the same latitude [5].

For the correct assessment of the climate-driven dynamics of the upper treeline, it is important to take into account the factors that limit the growth of forests. In previous publications about other mountain systems, researchers have identified different types of upper treelines—climatic and non-climatic [7]. It has been proposed to distinguish treelines originating due to the deterioration of thermal conditions with increases in elevation and impossible upright tree growth (thermal treeline) and others that constrain the existence of trees in some locations due to the absence of sufficient quantities of substrate (because of the wide spreading of stony fields), high water content in soil (bogs), or strong competition with grown vegetation for soil water and nutrients [12]. In some mountains at low latitudes (Southern Altay, Caucasus, Tien Shan), the spatial distribution of vegetation within the treeline ecotone is strongly linked to terrain parameters [13]. Thus, less solar radiation input results in a lower temperature and reduces the evapotranspiration on the northern slopes, leading to higher humidity and soil moisture and more widespread permafrost. The greater water availability favors the growth of trees [14]. Higher solar irradiation on southern slopes causes hydrological conditions that are too dry for the forests and thus support grassland [15].

In recent decades, attempts have been undertaken to estimate the structures of tree stands using remote sensing methods because repeated aerial photography and satellite imagery offer an excellent resource for the investigation of treeline shifts over wide territories. The indices of vegetation, like the most widely applied normalized differential vegetation index (NDVI), that are derived from multispectral satellite sensors (Landsat, MODIS, SPOT VGT) give us information about the "greenness" and vitality of the vegetation cover [13,16]. The NDVI also can be used for landscape mapping with the estimation of alpine forest structural variables from imaging spectrometer data [17].

The instrumental climate data from the weather stations of Altay and Western Sayan are often fragmentary and time series of climate parameters are not available for mountain sites as the climate stations usually are located near settlements in basins. Therefore, the representative climate data must be modeled by different types of regionalization processes [17].

As can be seen in previous studies, generally, the upward shift of a treeline is caused by a rise in air temperature. For instance, in the forest–tundra ecotone of Kuznetski

Alatau (adjacent to Altay from the north side), the upward shift of Siberian pine to higher elevations is related to a period of air temperature increase [18]. The rate of advancement of the treeline is 0.2–0.3 m/year in this region. The reaction of tree species to climate changes depends on the diversity of the ecological conditions, the level of phenotypic plasticity, and its possibility of modifying the environment. Moreover, the size of the mountains, absolute elevation, and distance from the sea are important variables [19]. The forest–tundra transition zone in the Western Sayan Mountains shows an upward shift of 0.6 m/year. In addition, it has been found that the shift is correlated with the temperature increasing and depends on the azimuth and slope steepness [20]. Klinge and colleagues also claimed that a low summer temperature mainly controls the upper treeline [16]. As can be seen, all the above works highlight the main role of the air temperature, and some authors have concluded that other factors (distance from the coastline, mass elevation effect, continentality, etc.) represent additional variables [5,21]. However, they do not fully explain the mechanics of the environmental processes that determine the treeline's elevational position.

With regard to the high rate of variation in the upper treeline position in similar latitudes in the Altay and Sayan Mountains, in our study, we investigated the past and present distribution of the open forest boundary and its relation to the actual climate and topography based on high-resolution satellite and climate data. In addition to the previous studies, we analyzed the specific impact of climate parameters related to the different slope aspects and edaphic conditions.

The following hypotheses were tested. (1) The variation in the elevation of the upper open forest boundary in similar latitudes is related to the summer air temperature and to the amount of direct solar radiation that the woody plants experience during the growth period. (2) At the landscape level, the difference in the elevation of the upper open forest boundary of the southern and northern slopes grows with an increase in insolation towards low latitudes. (3) The upward shift of the open forest boundary over the past 60 years has local specificity associated with the peculiarities of climatic changes.

2. Materials and Methods

2.1. Study Site

The study area covers the territory of the Altay Mountains, mostly located in the Russian Federation and particularly in the eastern part of Kazakhstan, and the Western Sayan Mountains—between 49°30′–53° N and 83°–94° E (see Figure 1).
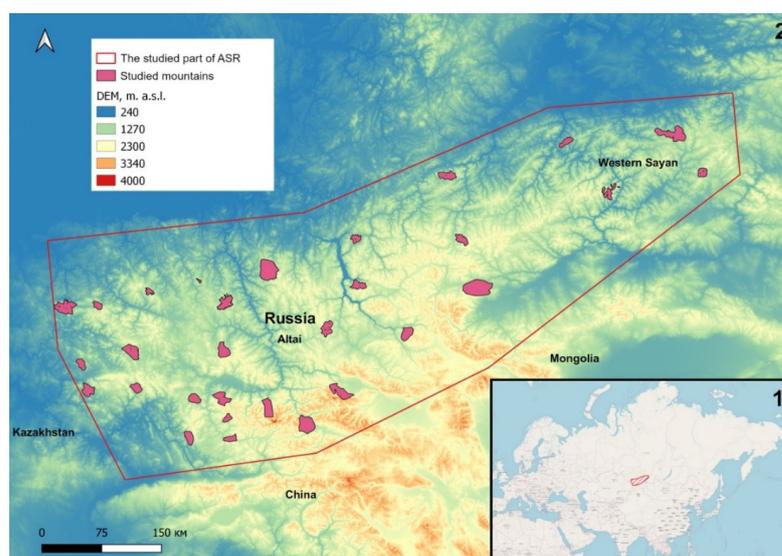

Figure 1. The study area within Eurasia (1) and the Altay and Sayan Mountain Region (2). Polygons demonstrate locations of 30 investigated mountains.

The study area is a vast territory located in the central part of Eurasia, at a great distance from both the Atlantic and the Arctic oceans. An assessment of the climate-driven dynamics of the upper boundary of the woody vegetation in this area is important (1) for an understanding of the prospects for the biodiversity of this region and to assess the consequences of such changes, (2) for comparison with similar processes in other mountainous regions of Eurasia (Alps, Khibiny, Caucasus, Ural Region, Putorana Plateau), and (3) to assess the global consequences of ecosystem changes.

The Altay Mountains are located in the south of the Western Siberian Plains and north of the Dzungarian and Gobi Deserts. In the northeast, the Altay Mountains are connected with the Western Sayan Mountains, and, in the southeast, they extend into the Gobi Altay. The mountain ranges rise from 1000 m a.s.l. in the northwest of the study area to more than 4500 m a.s.l. in the central part of the Russian Altay (Mt. Belukha). The western forelands of Altay are below 200 m. While the abrupt eroded valleys dominate the relief in the west and south of Altay, in the inland basins of the eastern part, widespread alluvial fans divide various mountain systems, most of which are isolated [16].

Altay and Western Sayan have an unequal distribution of precipitation and air temperature across the territory. The barriers of the Altay chains capture the precipitation of the wet air masses that arrive with the western cyclones. Precipitation mostly occurs in the short summer months from June to August. In the foothills and low mountains of Altay, from west to east, the average annual precipitation increases from 650 to 900 mm; further, as one moves deeper into the central part of Altay, the level of precipitation decreases to 300 mm [22]. This results in dry conditions in the eastern part of Altay. The northeast of Western Sayan is characterized by a large amount of precipitation in summer, with the bulk of the precipitation lingering on the northwestern macroslopes. With movement to the south, the amount of precipitation decreases in Western Sayan [23].

The temperature regime of the study area is also not uniform [24]. The highest average annual temperatures are typical for low-mountain areas, at 2.8 °C (Zmeinogorsk weather station, 355 m. a.s.l.); in the intermountain basins, this parameter drops to −0.3 °C (Ust-Koksa station, 978 m. a.s.l.), and, at higher stations, the temperature drops to −4.4 °C (Kosh-Agach weather station, 1758 m. a.s.l.). During summer, the daily maximum temperature in the central part of Altay can reach up to 40 °C, while, in winter, the daily minimum temperature is approximately −50 °C, which is characteristic of an extreme continental climate. During wintertime, the climate in Altay is controlled by the high-pressure cell, resulting in autochthonous cold and dry weather situations with temperature inversion and cold air in the basins. The weather stations indicate that the mean annual air temperature ranges between 6 and 7 °C [16].

The dominant species of forest in the study area are coniferous trees: Scots pine (*Pinus sylvestris* L.), Stone pine (*Pinus sibirica* Du Tour), Siberian fir (*Abies sibirica* Ledeb.), Siberian spruce (*Picea obovata* Ledeb.), and Siberian larch (*Larix sibirica* Ledeb.). Fir forests are mainly present in Northeastern Altay. In Northern Altay, spruce forests are widespread along the floodplains and on the first terrace almost everywhere. Stone pine forests usually grow on the upper part of the forest belt and represent the treeline. In Central and Southern Altay, larch trees establish forests on north-facing slopes and the lower forest belt on the southern slopes. In the upper parts of the mountains, the tree communities change to stone pine mixed with larch. The mixed coniferous taiga is prevalent in the Western Sayan Mountains. The mixed taiga also occupies the upper forest boundary. In some locations, where larch trees grow to the top from the north side, they can extend over the ridge and establish themselves in the highest parts of the southern slopes. The forests located in the southern part of the study area are limited to the slopes facing north, while the south-facing slopes are covered by mountain–steppe. Only larch trees are able to grow in these north-facing forest areas, located south of approximately 50.5° N. The soil temperature and water supply differ due to the varying solar radiation from the slope aspect, with less transpiration occurring in the northern aspects [16].

2.2. Estimation of Upper Open Forest Boundary Position for 1960s

The estimation of the upper open forest boundary position (crown closure > 10%) was performed in the 30 mountains systematically dispersed in the territory of Altay and Western Sayan (see Figure 1). For each surveyed mountain, using the historical topographic maps, with a scale of 1:50,000, a single polygon of the forest and the open forest boundaries were obtained for the 1960s. In this case, the georeferenced topographic map raster was also loaded into SAGA GIS (Open Source Software, University of Hamburg, Germany), where the areas with woody vegetation were automatically digitalized. To obtain a more consolidated upper treeline, for each vertex, the corresponding polygons were converted into a layer of points; then, all the points were connected by lines of length $\leq$ 60 m using Delaunay triangulation in QGIS (Open Source Software). This linear layer was converted into a single polygon, limiting the zone of distribution of closed and open forests in the 1960s (Figure 2).
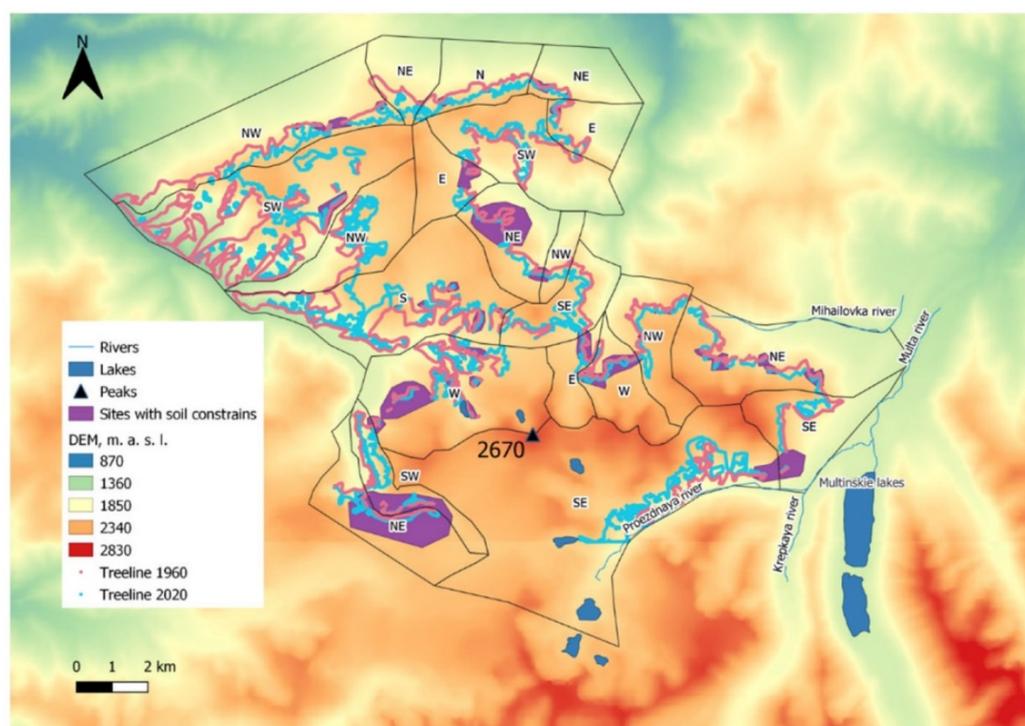

Figure 2. The upper open forest boundaries in 1960 and 2020 at different slope aspects and edaphic conditions on the slopes of Kholodnyi Belok Ridge (Central Altay).

2.3. Estimation of Contemporary Open Forest Boundary Position

For all 30 studied mountains in Altay and Western Sayan, the interpretation and study of the contours of plant communities were carried out with the use of contemporary Sentinel-2 satellite images (provided by European Space Agency, 2018–2022 observations, channels 1–12, NDVI layers). For each mountain, we used scenes from the growing season (July or early August) and early September [25].

In SAGA GIS, an unsupervised classification procedure was carried out, according to the K-Means algorithm, by the Iterative Min Distance method. The result was a raster containing 14 undefined categories of land features. Next, the vectorization of the raster was carried out, as a result of which a vector polygonal layer was obtained. Some of the polygons from this layer were used as signature samples for supervised classification in SAGA GIS. As a result, we determined the boundaries of the following landscape types: water bodies, shadows, dense forest, open forest, sparse tree stands, herbaceous vegetation on the tops of slopes, meadows, shrubs, rocks and stony fields, and tundra.

As a result, vector maps of the distribution of open forests (crown closure > 10%) were obtained. In order to obtain a consolidated open forest boundary (OFB) line, we also connected them by lines of length ≤ 60 m using Delaunay triangulation, and we obtained a single polygon of the zone of distribution of open forests in 2020.

2.4. Estimation of Shift in Open Forest Boundary Position for Period 1960–2020

The polygon of the OFB shift was obtained by the polygonal layer intersection of the OFB of the 1960s and 2020. It was used to calculate the shift area. The areas not occupied by trees and more than 1 hectare inside the shift area were excluded. Based on high-resolution images from open sources (Google (Mountain View, CA, USA), ArcGis MapServer (ESRI, Toronto, ON, Canada)), the visual correction of the contemporary boundaries of this polygon was carried out. The same images were used to identify the polygons of the areas where the position of the upper treeline was presumably affected by the unfavorable edaphic constraints (waterlogged soils, moraine deposits, or boulder fields).

Using DEMs (SRTM, spatial resolution 30 m/pix), the polygons of the 30 studied mountains were divided into macroslopes, according to the prevailing slope exposure (southeast, south, southwest, west, northwest, north, northeast, east) (see Figure 2).

To calculate the elevational shift, the contemporary open forest boundary lines and the lines of the 1960s were selected from the polygon of the OFB shift. These lines were converted into a layer of points with an interval of 12 m. The attributes of this layer included information about the exposure of the macroslope, the influence of soil conditions, and elevation. The terrain parameters were derived from the corresponding rasters and polygons, using the Point Sampling Tool module in QGIS.

Moreover, the average elevation of the OFB in the 1960s and 2020 and its shift over the past 60 years (Table S1) were calculated, for different slopes and edaphic conditions (Table S2). Horizontal and areal shifts were also calculated.

We interpolated the position data of the upper OFB of the 30 mountains using ordinary kriging in SAGA GIS.

2.5. Modeling of Spatial Pattern of Climate Parameters

According to the data from 339 weather stations (provided by A.N. Afonin for the period 1964–1974), the distribution surface of the sum of precipitation in the summer months was constructed. To create a raster layer of precipitation, we used the residual kriging method [26].

The calculated raster of the sum of precipitation was derived in SAGA GIS, according to a multiple regression formula (Equation (1), $R^2 = 0.38$). The values of the DEMs (resolution 500 m/pix) were submitted as the variables.

The differences between the actual and calculated values were taken as residuals. They were interpolated over the entire area of the raster (ordinary kriging) and used for the correction of the values calculated by Equation (1).

$$PCsu = 31.45 + 0.1 \times H \text{ - } 3.86 \times X + 9.47 \times Y \tag{1}$$

where *PCsu*—sum of adjusted summer precipitation (mm), *H*—elevation (m a.s.l.), *X*—longitude, *Y*—latitude.

Using the data on the summer sunshine duration (SD) and precipitation for 5 mountain regional weather stations for 1960–2020, we obtained a regression equation (Equation (2), $R^2 = 0.61$, Figure 3).

$$SD = 4049.9 \times PCsu - 0.299 \tag{2}$$

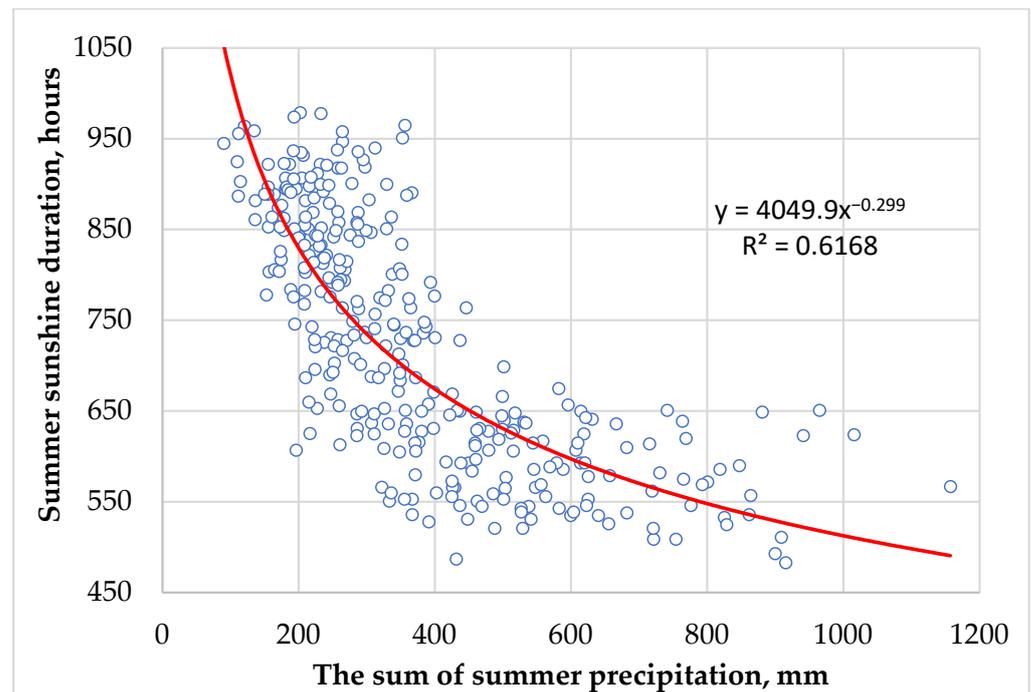where *SD*—the total summer sunshine duration, *PCsu*—the sum of summer precipitation (mm).

Figure 3. Ratio of summer sunshine duration to the amount of precipitation in 1960–2020.

According to Equation (2) and the values of the precipitation raster, we derived the raster of the summer sunshine duration.

Using data on the summer temperature from 268 weather stations, a regression equation (Equation (3)) was obtained for the dependence of the temperature on the elevation above sea level and on the latitude and longitude of the location. In addition, using residual kriging, the surface of the distribution of the summer temperature was obtained.

$$Tsu = 47.35 - 0.004 \times H - 0.08 \times X - 0.4 \times Y \tag{3}$$

where *H*—the elevation of the weather station (m a.s.l.), *X*—longitude (decimal degrees), *Y*—latitude (decimal degrees).

In QGIS, from the corresponding rasters inside the 30 polygons of the boundaries of the studied mountains, the median values of the following were obtained: the elevational position of the OFB in the 1960s and 2020, the temperature in 1964–1974, and the sum of precipitation separately for the summer and winter periods in 1964–1974.

3. Results

3.1. The Open Forest Boundaries' Positions in the 1960s

The spatial analysis of the open forest boundaries in the 1960s in all 30 studied mountains showed that in the western parts of Altay, their mean elevational positions were lower than at the inner part (1300–1600 vs. 1700–2200 m a.s.l.) (Figure 4). A similar increase in the OFB position was revealed when moving from the northern to the central part of Altay (from 1600–1800 up to 2100–2200 m a.s.l.) and from the northern to the southern part of the Western Sayan Mountains (from 1400–1600 up to 1900–2000 m a.s.l.) (Figure 4).
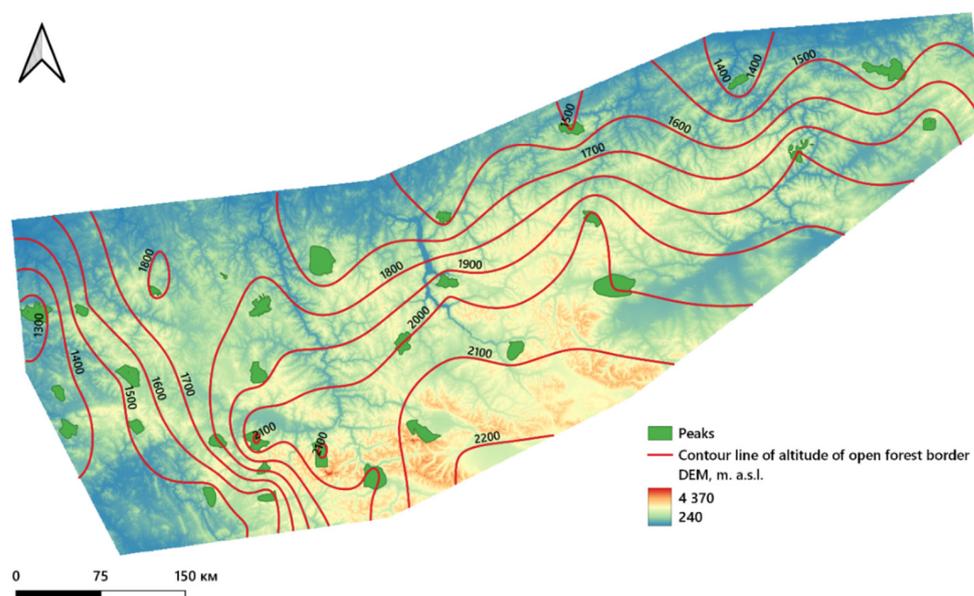
Figure 4. The mean elevational position of the open forest boundary in the 1960s (red contour lines) in Altay and Western Sayan.

3.2. Elevation of Open Forest Boundary in 1960s at Different Latitudes and Slope Aspects

Since there are great differences of soil wetness and the development of ground vegetation on the southern and the northern slopes of the study area [14,15], we calculated the ratio between the elevation of the open forest boundary on such opposite slopes. The comparison of the elevational position of the OFB at different slopes of the 30 studied mountains demonstrated that at latitudes close to 50°10′ N, the elevation of the upper OFB on the southern exposures was less than on the northern ones. This led to the variation in this ratio from 0.79 to 0.95. At higher latitudes (51–53 °N), this ratio had values mostly greater than 0.95 (Figure 5, Table S1, and Figure S1).
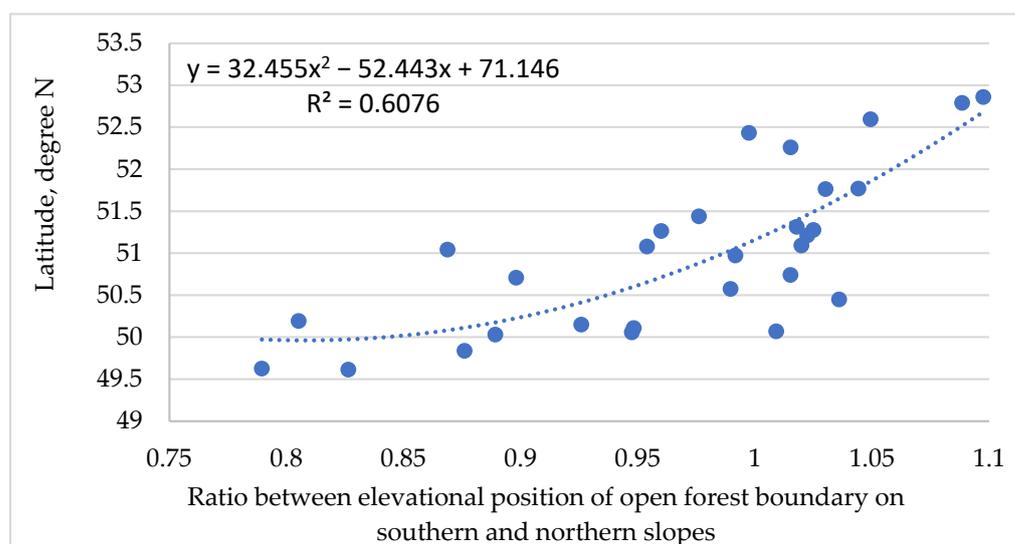

Figure 5. Latitudinal changes in the ratio between elevational position of the open forest boundary on southern and northern slopes of studied mountains in Altay and Western Sayan.

3.3. Spatial Distribution of Air Temperature, Precipitation, and Sunshine Duration in Study Area

The interpolated values of the mean summer air temperature for the summer season in the study area were between 2 and 22 °C in 1964–1974 (Figure 6). The highest temperatures (16–22 °C) were recorded in the western and southern foothills of Altay. The same values

were obtained for the northern and southern parts of Western Sayan. An air temperature between 2 and 16 °C is typical for highlands in the central parts of the study area.
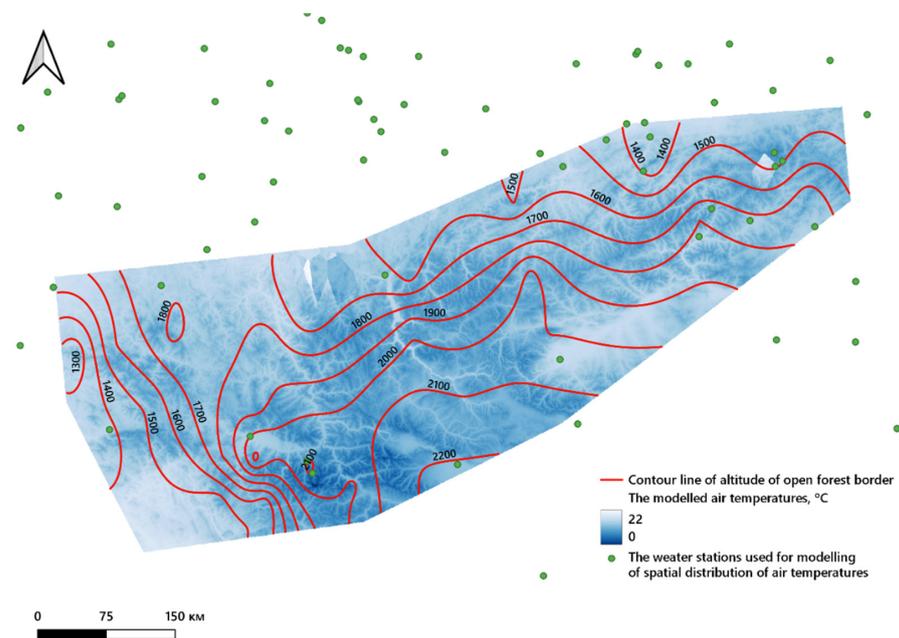

Figure 6. The June–August air temperature (°C) in Altay and Western Sayan modeled using elevation and geographic coordinates. Green points—71 nearest weather stations used for modeling of the spatial distribution of temperature (total count 268). The red contour lines represent the mean elevational position of the open forest boundary in the 1960s.

In the 1960s, the largest amount of precipitation (390–600 mm) occurred in the western and the northern parts of Altay and Western Sayan. In the inner parts of the, the precipitation was less than 300 mm (Figure 7).
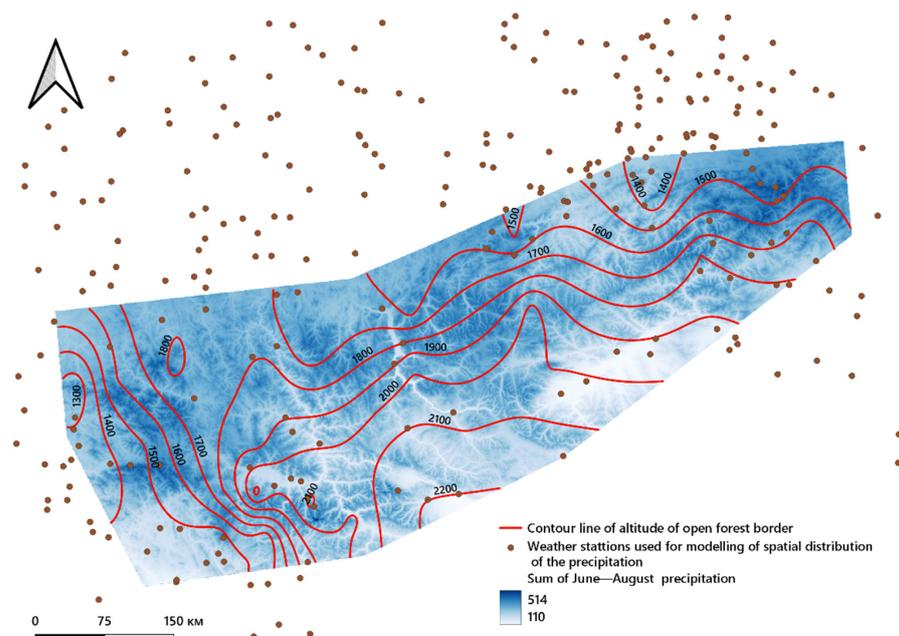

Figure 7. Sum of June–August precipitation (mm) in Altay and Western Sayan modeled using elevation and geographic coordinates. Brown points—274 nearest weather stations used for modeling of spatial distribution of precipitation (total count 339). The red contour lines represent the mean elevational position of the open forest boundary in the 1960s.

The longest sunshine duration in the study area was recognized in the central parts (860–1000 h). In the western and the northern parts of Altay and in the northern part of Western Sayan, this climatic parameter was less than 860 h (Figure 8).
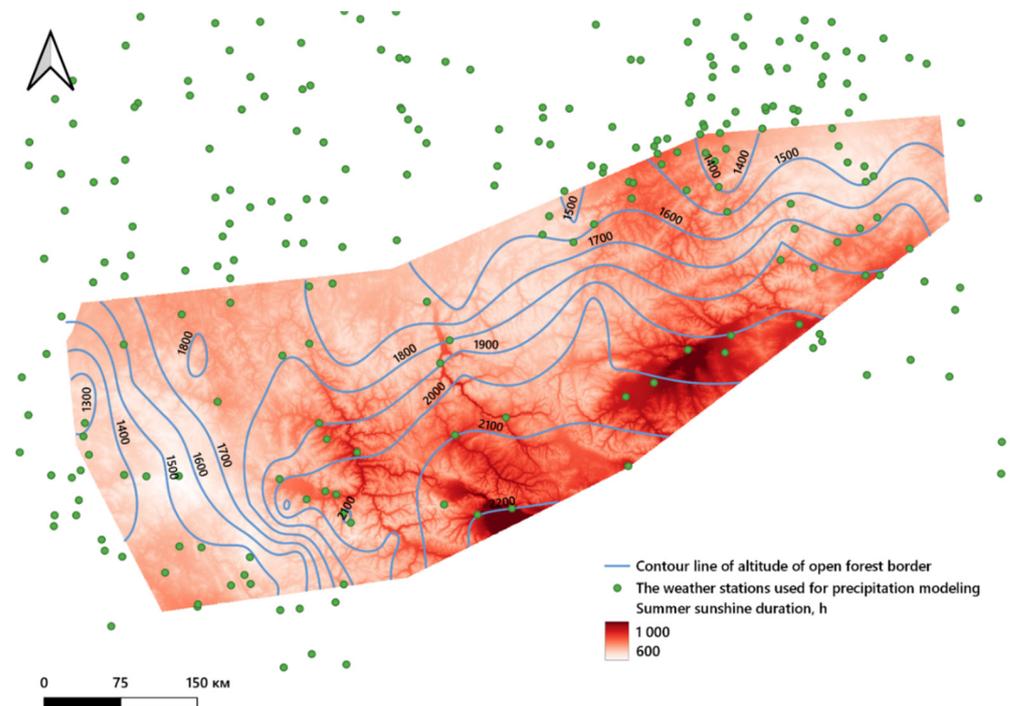

Figure 8. Sum of June–August sunshine duration in Altay and Western Sayan (hours). Green points—274 nearest weather stations used for modeling of the spatial distribution of sunshine duration (total count 339). The blue contour lines represent the mean elevational position of the open forest boundary in the 1960s.

3.4. Relationship between Climatic Parameters and the Elevational Position of the Open Forest Boundary in the 1960s

The analysis of the relations between single climatic parameters and the elevational position of the OFB in the 1960s has shown that on the studied mountains, with movement from the outer to the inner parts of Altay and Western Sayan, the summer air temperature and precipitation linearly decreased with the elevation of the OFB (see Figure 9A,B), but the summer sunshine duration increased (see Figure 9C). Thus, in the outer part of the studied mountains, where the OFB elevation was less than 1400 m a.s.l., the summer air temperature was 11–13 °C. However, in the inner mountains, with an OFB elevation of more than 2050 m a.s.l., the summer air temperature varied between 7.3 and 10 °C. At the same time, sum of June–August precipitation was 450–500 mm in the outer mountains, but 250–380 mm in the inner ones. In contrast, the sunshine duration was 620–650 h in the outer parts of the mountains and 730–775 h in the inner ones.

In the multiple regression analysis, including climatic parameters as independent variables and the OFB elevational position as a dependent variable, a significant relation (p-value < 0.05) was found only for the combination of air temperature and sunshine duration (see Table 1, Equation C). They explained 80% of the variance in the OFB position. At the elevation of the OFB, the air temperature and sunshine duration changed in the opposite manner—with the increase in OFB elevation, the air temperature decreased and the sunshine duration increased (see Figure 9D).
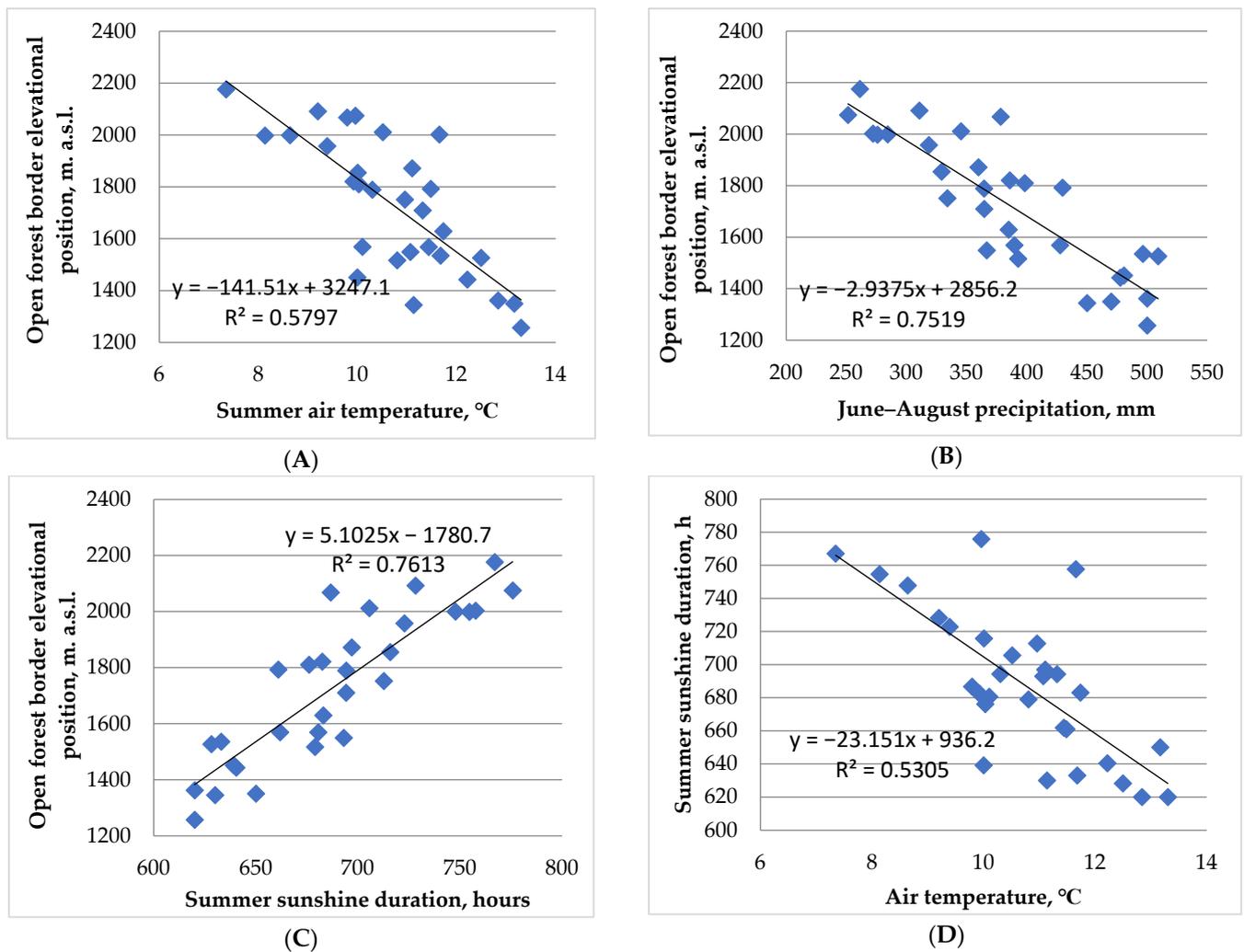
Figure 9. The relationship between mean air temperature, precipitation, summer sunshine duration, and open forest boundary elevational position (**A–C**) and air temperature and total summer sunshine duration (**D**) on studied mountains.

Table 1. The multiple linear regression analysis and coefficients in equation.

Equation	Free Term	Coefficients with Independent Variables					Multiply R	R^2
		Summer Air Temperature	Summer Sunshine Duration	Summer Precipitation	Winter Precipitation	Product of Air Temperature by Sunshine Duration		
A	1559.7	−37.50	1.70	−3.00	1.90		0.90	0.80
p-value		0.13	0.62	0.23	0.06			
B	−585.9	−50.02	4.10	0.08			0.89	0.80
p-value		0.05	0.24	0.97				
C	−461.1	−49.81	3.96				0.89	0.80
p-value		<0.05	<0.05					
D	1531.0	−232.28	1.13			0.26	0.89	0.80
p-value		0.31	0.75			0.42		

3.5. Open Forest Boundary Elevational Position in 2020

The spatial analysis of the open forest boundary in 2020 in all 30 studied mountains showed that in the western part of Altay, their mean elevational positions were lower than in the inner part (1500–1700 vs. 2100–2300 m a.s.l.) (Figure 10). The elevational position of

the OFB also increases when we move from the northern to the central part of Altay (from 1700–1900 up to 2200–2300 m a.s.l.) and from the northern to the southern part of Western Sayan (from 1500–1700 up to 1900–2000 m a.s.l.).
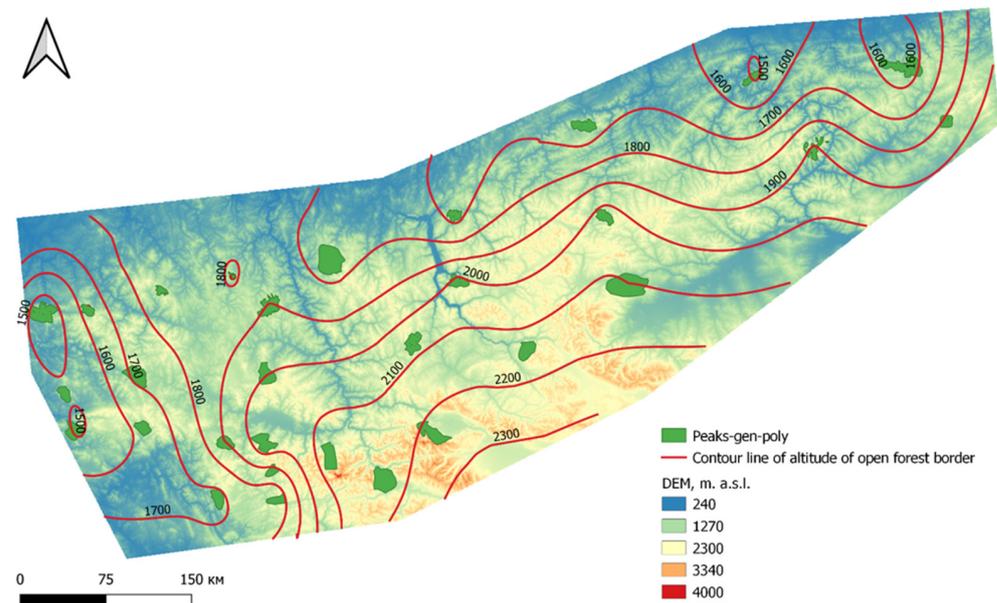

Figure 10. The mean elevational position of the open forest boundary in 2020 (red contour lines) in Altay and Western Sayan.

3.6. Elevation and Shifts in the OFB from 1960 to 2020 and Changes in the Areas Occupied by Woody Vegetation

We found that the highest elevational shift of the OFB since the 1960s occurred in the western part of Altay (100–130 m) and in the northern part of Western Sayan (100–110 m), and the smallest shifts in the northeastern part of Altay (80 m) (Figure 11).
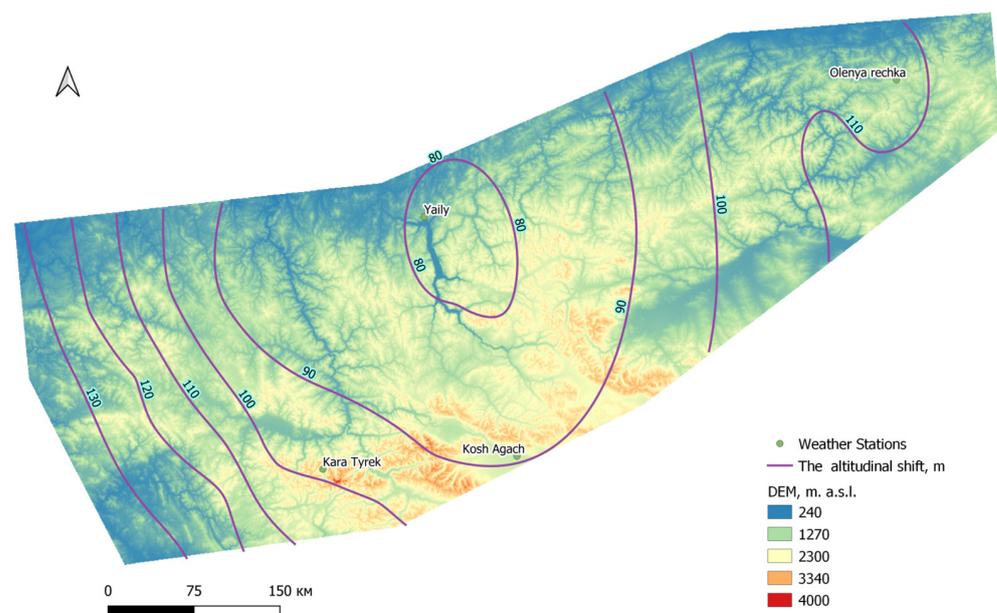

Figure 11. The spatial distribution of elevational shift values (m) in Altay–Sayan region.

In all 30 studied mountains, the values of the elevational shift were obtained from the median values of the upper treeline elevation, according to the exposures of the slopes (Table S2). The average value on the northern slopes (N, NE, NW) was 99 m. For the

southern slopes (S, SE, SW), it was 103 m (Table S1). The elevation shift was also estimated for slopes with edaphic constraints (Table S2). On the northern slopes with edaphic constraints, the elevational shift was 24 m, and that on the southern slopes was 23 m. The percentage of the slopes with a strong influence of waterlogged soils, moraine deposits, or boulder fields on tree stand dynamics was approximately 16%.

The area occupied by woody vegetation also changed. The average shift area in the northern direction was 15.9 ha per 1 km of borderline in the 1960s; in the southern direction, it was 17.5 ha per 1 km (see Table 2). The change in the area occupied by forests in the southern exposures was greater than in the northern ones. The change in area was greater than the change in the elevation of the OFB (Table 2).

Table 2. The area of the OFB shift zone for different aspects.

Aspect	Average Shift Area, ha	Mean of Shift Area per 1 km of Borderline in 1960s, ha
E	302.0	15.1
N	397.7	17.3
NE	397.3	15.3
NW	422.3	15.1
Mean N-NE-NW	405.8	15.9
S	409.6	17.8
SE	517.0	18.5
SW	531.1	19.0
W	348.4	15.2
Mean S-SE-SW	465.5	17.5

3.7. Changes in Climate Variables in Study Area in 1960–2020

The analysis of climatic data collected at four mountain weather stations (Oleniya rechka, Kara-Turek, Kosh-Agach, and Yaily) (see locations in Figure 11) demonstrated that in 1960–2020, the summer air temperature increased in the outer part of the study area (Oleniya rechka and Yaily) by 1.8 °C and in the inner part (Kara-Turek, Kosh-Agach) by 2.4 °C (0.3–0.4 °C per decade) (Figure 12A) [27].

At the same time, the summer precipitation has been decreasing on average by 6.3 mm each decade at the Oleniya rechka weather station (which had the highest level of summer precipitation) and varying without any tendency at the Kara-Turek, Yaily (moderate level of summer precipitation), and Kosh-Agach (lower level of summer precipitation) weather stations (Figure 12B). The summer sunshine duration for the period of 60 years at the Oleniya Rechka and Yaily weather stations increased by 24.6 h (4.3%) and 53.0 h (7.9%), respectively (Figure 12C). For the inner weather stations at Kara Tyrek and Kosh-Agach, the summer sunshine duration increased by 108 and 120 h or 14.5% and 16% in relation to the starting value in the 1960s, respectively.

3.8. Model Evaluation

For model C in Table 1, a cross-validation procedure (Scikit-learn library for Python) was performed [28]. The average mean absolute error (number of folds: 30) was equal to 103.1 m.

Moreover, in accordance with the climate parameters of 2020 for two mountain weather stations (Olenya Rechka and Kara-Tyrek) and Equation C (see Table 1), the predicted OFB elevation was calculated. In comparison with the elevational position obtained from the satellite images in 2020, the absolute error was 1.1 m for Olenya Rechka (Ergaki mountain) and 53.5 m for Kara-Tyrek.
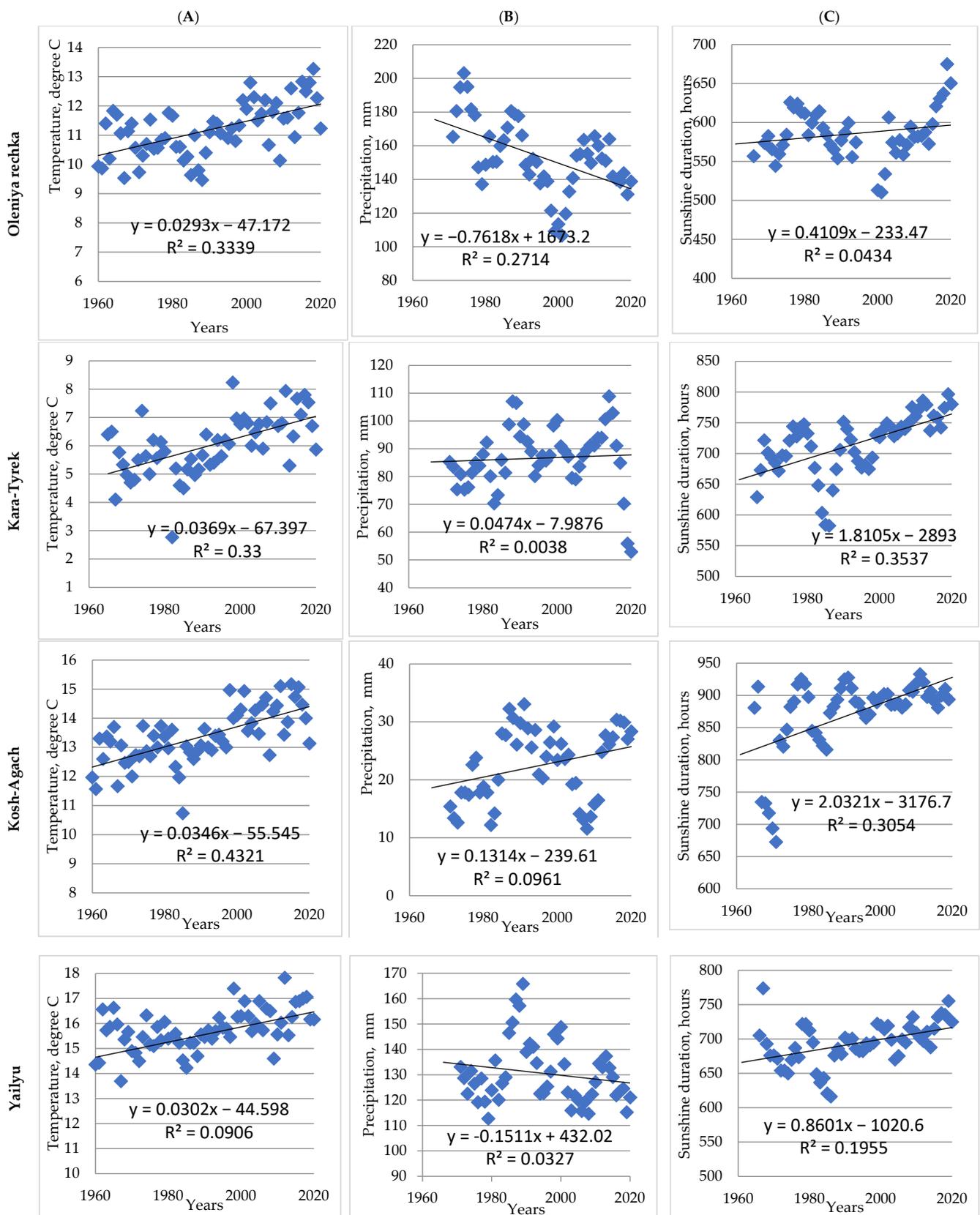
Figure 12. Changes in climatic parameters in 1960–2020 according to the data collected at the weather stations at Oleniya rechka and Yailyu (higher level of summer precipitation), Kara-Tyrek (moderate level of summer precipitation), and Kosh-Agach (lower level of summer precipitation): (**A**) summer temperature; (**B**) running mean of summer precipitation; (**C**) summer sunshine duration.

4. Discussion

4.1. Reasons for Spatial Variation in Open Forest Boundary Elevation in Altay and Western Sayan

Our results show that the OFB in Altay and Western Sayan reached the maximal elevation (more than 2000 m a.s.l.) at the locations with minimal precipitation and summer air temperatures and the maximal sunshine duration (see Figure 9). In the mountains, where the summer air temperature and precipitation are higher, the OFB was at elevation 1300–1500 m a.s.l. In locations with a large amount of precipitation, the greater cloudiness decreases heating, caused by the direct solar radiation of the Earth's surface and vegetation. Subsequently, it restricts the establishment and growth of woody plants at higher elevations in the mountains, even if the summer air temperatures are quite high.

In previous publications, it has been pointed out also that, at similar latitudes, the upper treeline is located at a higher elevation in the interior than in the outer parts of he mountain system. This has been related to the mass elevation effect (MEE). In the Bolivian Andes, in the more arid highlands, the upper treeline reaches elevations of 4800–4900 m above sea level due to the longer periods of sunshine [5]. Moreover, in the United States of America, it is noted that at the same latitude, in more humid western areas, the treeline limit is located at a lower position compared to drier continental areas [29].

In the Swiss Alps, the summer air temperatures are lower in the inner and higher in the outer part (Weissfluhjoch, 2690 m, daily mean 5.6 °C; Samedan, 1709 m, 11.5 °C; Scuol, 1304 m, 13.2 °C; Buchs/Aarau, 387 m, 17.3 °C) (MeteoSwiss). Moreover, the Central Alps have a higher sunshine duration value (Meteoswiss) [30]. At the same time, the treeline elevation is higher in the inner part of the Alps: 2219 m a.s.l. at Valais, 2294 m a.s.l. at Engadin, and 2142 m a.s.l. at the Southern Alps [31].

The MEE was proposed more than a century ago by A. de Quervain in 1904 to describe the tendency of the snowline and the treeline to occupy higher elevations in the Central Alps than in their outskirts [32]. The phenomenon of the MEE was explained by Brockmann-Jerosch (1919) as the result of the thermodynamic effect of mountain masses [33]. The temperature difference between the inner and outer parts of a mountain system is essential for the MEE and has been defined as the real value of the MEE [34]. The MEE is an aspect of the continental climate and will expand with the spatial extent of high mountain ranges. Severin Irl and colleagues (2016) claimed that the causes of the MEE are minor cloudiness, higher insolation, and therefore higher temperatures at a given elevation and latitude inside mountain ranges compared to single mountains [35]. Such thermal advantages create favorable growing conditions for trees at higher elevations [36]. Christian Körner (2012) explained the MEE as the cooling of air masses, condensation of moisture, formation of clouds, and precipitation at the periphery of a mountain system. Hence, the inner part of the mountain is drier and receives more sunshine hours. Moreover, the combination of slope warming, due to enhanced irradiation, and reduced evaporative cooling causes a shift in isotherms and treelines to higher elevations in the central parts of mountain systems [5]. David Kienle and colleagues (2023) expressed the MEE as a proxy variable by means of the distance to the mountain chain outline or distance from the coastline [21].

As has been demonstrated above, most researchers claim that cloudiness in the central parts of large mountain systems is reduced and it causes the air temperature to increase. This leads to a shift to higher elevations for isotherms and temperature-dependent tree-lines [5,21,35]. Our results demonstrate that with movement from the outer to the inner parts of the Altay and Western Sayan Mountains, the air temperature on the upper OFB falls by 5–6 °C; however, the difference expected due to the previous explanation of the MEE should be close to zero. Based on our results, we claim that the MEE increases not only the air temperature, but mostly the surface temperature (including the surfaces of the tree parts—leaves, branches, trunks), since irradiation grows when the sunshine duration increases at the same elevation in the central parts of the study area. The combination of the air temperature and sunshine duration predicts better the mean elevation position of the OFB inside our study area (see Table 1). We have calculated that the increase in sunshine to 23 h during the summer months compensates for the decrease in the air temperature of

1 °C when the OFB shifts at 153 m elevation with movement from the outer to the inner part of the study area (see Figure 9D). We believe that the MEE should be taken into account as a predictor of the upper treeline position in any region, but it is better represented as the summer sunshine duration instead of continentality or distance from the coastline, as has been proposed by David Kienle and colleagues (2023) [21].

4.2. Elevation of Upper Open Forest Boundary on Southern and Northern Slopes

It should be noted that within the study area, a small latitudinal gradient (49.6–52.9 degrees) takes place. This, in our opinion, determines the difference in the elevation position of the upper OFB of the north-facing and the south-facing exposures for mountains located along this gradient and can be explained by a larger solar incidence angle at southern part of the study area. This leads to the fact that, under comparable levels of precipitation and sunshine duration, the south-facing slopes of the mountains at a latitude less than 50°10′ N are heated up more and lose more moisture than south-facing slopes at latitudes more than 51° N. We calculated that the ratio of the OFB elevational position on south- and north-facing slopes is less than 1.0 in the southern parts and more than 1.0 in the northern parts of the study area (Figure S1). The lack of moisture is an obstacle to the resettlement of the woody vegetation, as was revealed in the research of M. Beloiu and colleagues (2022) and C. Dulamsuren and colleagues (2010) [37,38]. We claim that the difference in the elevation of the upper OFB for south-facing and north-facing slopes grows with the increase in insolation and with the decrease in latitude in our study area.

4.3. The Upward Shift of the Open Forest Boundary over the Past 60 Years

Our findings confirm that the forest's advance to the mountains could be significantly limited by unfavorable edaphic conditions and unsuitable substrates [39–42]. Thus, on the studied mountains in Altay and Western Sayan, the open forest boundary shifted four times less in the sites with widespread boulder fields, moraine deposits, and waterlogged soils than in sites without them (see Table S2).

Our results demonstrate that the OFB shifted by 80–130 m upslope on sites without edaphic constraints in the last 60 years in the study area (Figure 11). We suppose that the main drivers, as mentioned in previous publications, were changes in the summer temperature, which increased by 1.8–2.4 °C in Altay and Western Sayan (Figure 12). However, the most significant elevational shift of the upper OFB (110–130 m) occurred in the highly humid parts of Western Altay and Northeastern Western Sayan. We assume that this is due to the decrease in summer precipitation by 22%, which significantly reduced evaporative cooling, and a slight (4.3%) increase in the sunshine duration (see data collected from Oleniya rechka weather station in Figure 12). In the parts where a moderate shift was revealed (approximately 100 m a.s.l.), we suppose that an additional driver of the forest's advance, besides the rise in the summer temperature, was the increase in the sunshine duration by 14% (see data from Kara-Turek weather station in Figure 12), because precipitation fluctuated without any tendency there. Previous works described a similar increase in the sunshine duration and related air temperature over the period of 1980–2020 across Europe, caused by the brightening phenomenon [39]. We consider that in the inner arid part of the study area, surrounding the weather station at Kosh-Agach, the slight rise in precipitation and the significant increase in the sunshine duration (16%) caused the shift in the OFB elevation of 90 m (see data on Figure 12). A minimal elevational shift in the upper OFB (approximately 80 m) occurred in the humid northeastern parts of Altay, where slight changes in summer precipitation and sunshine duration were observed (see data from Yailyu weather station in Figure 12). We suppose that the upward shift of the treeline over the past 60 years has local specificity associated with the peculiarities of the climatic changes in different parts of Altay and Western Sayan. The spatial variation in the OFB shift inside the study area also confirms that the elevational position of the upper climate-dependent treeline was determined not only by changes in the summer air temperature but also by the sunshine duration and precipitation. Additionally, the evaluation of the model

(Equation C, Table 1) for OFB calculation shows that it needs to be improved by including new data samples from other mountains in this region. The lack of climatic data can be rectified by using contemporary satellite data.

5. Conclusions

Our study of spatial variations in the open forest boundary elevational position in the Altay and Western Sayan Mountains in the 1960s shows that it has been determined not only by the summer air temperature, but also by the sunshine duration and precipitation. We also have revealed that a higher insolation level determines a decline in the open forest boundary elevation on south-facing slopes in the southern part of the study area, despite the similar level of precipitation and sunshine duration. Our spatiotemporal analysis of the OFB shift (80–130 m of elevation) in the mountains in the southern part of Central Siberia demonstrates that it depends on combined changes in the summer air temperature, sunshine duration, and precipitation. The treeline advances are closely related to the higher absorption of solar radiation in newly forested areas and changes in carbon sequestration in plants and soils; thus, data about the climate effects on the tree stand distribution and dynamics at the upper limit of their growth, obtained by us, could be implemented for a more precise assessment of global warming processes. We suppose that a deeper understanding of the climatic factors that affect tree stand dynamics, based on a modeling approach that integrates climate, edaphic conditions, and topographic features (slope exposition), would be highly helpful for the improvement of predictions of tree stand responses to the climatic changes in mountainous regions.

Supplementary Materials: The following supporting information can be downloaded at: https://www.mdpi.com/article/10.3390/f14101987/s1, Figure S1: The values of OFBpos_S/OFBpos_N for 30 summits, the summer sunshine duration, and the geographic positions; Table S1: Altitudinal position and shift of OFB in 1960 and 2020; Table S2: Altitudinal shifts for period of 1960–2020 for sites with and without soil constraints and average shift in ASR.

Author Contributions: P.A.M. conceived and coordinated the overall project. N.F.N. collected and treated the materials and analyzed the data. P.A.M. and N.F.N. prepared the tables and figures and wrote the manuscript. All authors have read and agreed to the published version of the manuscript.

Institutional Review Board Statement: Not applicable.

Informed Consent Statement: Not applicable.

Data Availability Statement: The data presented in this study are available on request from the corresponding author.

Conflicts of Interest: The authors declare no conflict of interest. The funders had no role in the design of the study; in the collection, analyses, or interpretation of the data; in the writing of the manuscript; or in the decision to publish the results.

References

1. Masson-Delmotte, V.; Zhai, P.; Pirani, A.; Connors, S.L.; Péan, C.; Berger, S.; Caud, N.; Chen, Y.; Goldfarb, L.; Gomis, M.I.; et al. (Eds.) Contribution of Working Group I to the Sixth Assessment Report of the Intergovernmental Panel on Climate Change. In *Climate Change 2021: The Physical Science Basis*; Cambridge University Press: Cambridge, UK; New York, NY, USA, 2021.
2. Churakova-Sidorova, O.V.; Myglan, V.S.; Fonti, M.V.; Naumova, O.V.; Kirdyanov, A.V.; Kalugin, I.A.; Babich, V.V.; Falster, G.M.; Vaganov, E.A.; Siegwolf, R.T.W.; et al. Modern aridity in the Altai-Sayan mountain range derived from multiple millennial proxies. *Sci. Rep.* **2022**, *12*, 7752. [CrossRef] [PubMed]
3. Li, Y.; Zhang, D.; Andreeva, M.; Li, Y.; Fan, L.; Tang, M. Temporal-spatial variability of modern climate in the Altai Mountains during 1970–2015. *PLoS ONE* **2020**, *15*, e0230196. [CrossRef] [PubMed]
4. Körner, C. Carbon limitation in trees. *J. Ecol.* **2003**, *91*, 4–17. [CrossRef]
5. Körner, C. *Alpine Treelines*; Springer: Basel, Switzerland, 2012; ISBN 978-3-0348-0395-3.
6. Holtmeier, F.K.; Broll, G. Treeline research-from the roots of the past to present time: A review. *Forests* **2020**, *11*, 38. [CrossRef]
7. Holtmeier, F.-K. *Mountain Timberlines: Ecology, Patchiness, and Dynamics*; Springer Science & Business Media: Berlin/Heidelberg, Germany, 2009; ISBN 978-1-4020-9705-8.

8.   Paulsen, J.; Körner, C. A climate-based model to predict potential treeline position around the globe. *Alp. Bot.* **2014**, *124*, 1–12. [CrossRef]

9.   Scherrer, D.; Körner, C. Infra-red thermometry of alpine landscapes challenges climatic warming projections. *Glob. Chang. Biol.* **2010**, *16*, 2602–2613. [CrossRef]

10.   Jobbágy Esteban, G.; Jackson, R.B. Global controls of forest line elevation in the northern and southern hemispheres. *Glob. Ecol. Biogeogr.* **2000**, *9*, 253–268. [CrossRef]

11.   Klinge, M.; Dulamsuren, C.; Erasmi, S.; Karger, D.N.; Hauck, M. Climate effects on vegetation vitality at the treeline of boreal forests of Mongolia. *Biogeosciences* **2018**, *15*, 1319–1333. [CrossRef]

12.   Gorchakovsky, P.L.; Shiyatov, S.G. *Phytoindication of Environmental Conditions and Natural Processes in High Mountains*; Nauka: Moskow, Russia, 1985.

13.   Klinge, M.; Böhner, J.; Erasmi, S. Modeling forest lines and forest distribution patterns with remote-sensing data in a mountainous region of semiarid central Asia. *Biogeosciences* **2015**, *12*, 2893–2905. [CrossRef]

14.   Dashtseren, A.; Ishikawa, M.; Iijima, Y.; Jambaljav, Y. Temperature Regimes of the Active Layer and Seasonally Frozen Ground under a Forest-Steppe Mosaic, Mongolia: Temperature Regimes of the Active Layer and Seasonally Frozen Ground, Mongolia. *Permafr. Periglac. Process.* **2014**, *25*, 295–306. [CrossRef]

15.   Måren, I.E.; Karki, S.; Prajapati, C.; Yadav, R.K.; Shrestha, B.B. Facing north or south: Does slope aspect impact forest stand characteristics and soil properties in a semiarid trans-Himalayan valley? *J. Arid Environ.* **2015**, *121*, 112–123. [CrossRef]

16.   Klinge, M.; Böhner, J.; Lehmkuhl, F. Climate pattern, snow- and timberlines in the Altai Mountains, Central Asia. *Erdkunde* **2003**, *57*, 296–307. [CrossRef]

17.   Böhner, J.; Selige, T. Spatial prediction of soil attributes using terrain analysis and climate regionalization. *Gott. Geograpihsche Abh.* **2002**, *115*, 13–27.

18.   Petrov, I.A.; Shushpanov, A.S.; Golyukov, A.S.; Kharuk, V.I. Pinus sibirica Du Tour response to climate change in the forests of the kuznetsk alatau mountains. *Sib. J. For. Sci.* **2019**, *5*, 43–53. [CrossRef]

19.   Khutornoy, O.V. Structure and dynamics of conifers tree line in the mountains of southern siberia. *Proc. Tigirek State Nat. Reserv.* **2015**, *7*, 210–215. [CrossRef]

20.   Kharuk, V.I.; Im, S.T.; Dvinskaya, M.L. Forest-tundra ecotone response to climate change in the Western Sayan Mountains, Siberia. *Scand. J. For. Res.* **2010**, *25*, 224–233. [CrossRef]

21.   Kienle, D.R.; Irl, S.D.H.; Beierkuhnlein, C. Mass elevation effect and continentality have a stronger impact on global treelines than spatial isolation. *Glob. Ecol. Biogeogr.* **2023**, *32*, 1087–1097. [CrossRef]

22.   Kharlamova, N.; Kozlova, D. Statistical Characteristics of Atmospheric Precipitation Regime in the Altai Region. *News Altai State Univ.* **2014**, *1*, 145–150. [CrossRef]

23.   Pryakhina, G.V.; Zelepukina, E.S.; Osipova, T.N.; Gavrilkina, S.A.; Solovyev, V.A.; Vinogradova, T.A. Seasonal distribution patterns of precipitation on the territory of West Sayan ridge and taking them into account during the runoff modeling. *Vestn. Saint Petersbg. Univ. Earth Sci.* **2019**, *64*, 466–476. [CrossRef]

24.   Kharlamova, N. *Klimat Altaiskogo Regiona [Climate of Altay Region]*; Altay State University: Barnaul, Russia, 2013.

25.   Sinergise Ltd. EO Browser. Available online: https://www.sentinel-hub.com/explore/eobrowser (accessed on 16 August 2023).

26.   Hart, T.S.; Greene, S.L.; Afonin, A. Mapping for Germplasm Collections: Site Selection and Attribution. In Proceedings of the 3rd International Conference/Workshop on Integrating GIS and Environmental Modeling, Santa Fe, NM, USA, 21–25 January 1996; National Center for Geographic Information and Analysis (NCGIA): Santa Barbara, CA, USA, 1996.

27.   Veselov, V.; Pribilskaya, I.M.O. АИСОРИ. Available online: http://aisori-m.meteo.ru/waisori/ (accessed on 16 August 2023).

28.   Berrar, D. Cross-validation. *Encycl. Bioinforma. Comput. Biol. ABC Bioinform.* **2018**, *1–3*, 542–545. [CrossRef]

29.   Grafius, D.R. Distribution and Biomass Dynamics of the Alpine Treeline Ecotone Across the Western United States. Ph.D. Thesis, University of Iowa, Iowa City, IA, USA, 2012.

30.   Climate Diagrams and Normals per Station. Available online: https://www.meteoswiss.admin.ch/climate/the-climate-of-switzerland/climate-normals/climate-diagrams-and-normals-per-station.html (accessed on 16 August 2023).

31.   Szerencsits, E. Swiss Tree Lines—A GIS-Based Approximation. *Landsc. Online* **2012**, *28*, 1–18. [CrossRef]

32.   Quervain, A. *Die Hebung der Atmosphärischen Lsothermenin der Schweizer Alpen und ihre Beziehung zu deren Höhengrenzen*; Forgotten Books: Leipzig, Germany, 1904.

33.   Brockmann-Jerosch, H. *Baumgrenze und Klimacharakter. Beiträge zur geobotanischen Landesaufnahme 6*; Verlag von Rascher & Cie: Zurich, Switzerland, 1919; Volume 255.

34.   Zhang, B.; Yao, Y. Implications of mass elevation effect for the altitudinal patterns of global ecology. *J. Geogr. Sci.* **2016**, *26*, 871–877. [CrossRef]

35.   Irl, S.D.H.; Anthelme, F.; Harter, D.E.V.; Jentsch, A.; Lotter, E.; Steinbauer, M.J.; Beierkuhnlein, C. Patterns of island treeline elevation—A global perspective. *Ecography (Cop.)* **2016**, *39*, 427–436. [CrossRef]

36.   Troll, C. The Upper Timberlines in Different Climatic Zones. *Arct. Alp. Res.* **1973**, *5*, 3–18.

37.   Beloiu, M.; Poursanidis, D.; Tsakirakis, A.; Chrysoulakis, N.; Hoffmann, S.; Lymberakis, P.; Barnias, A.; Kienle, D.; Beierkuhnlein, C. No treeline shift despite climate change over the last 70 years. *For. Ecosyst.* **2022**, *9*, 100002. [CrossRef]

38.   Dulamsuren, C.; Hauck, M.; Khishigjargal, M.; Leuschner, H.H.; Leuschner, C. Diverging climate trends in Mongolian taiga forests influence growth and regeneration of Larix sibirica. *Oecologia* **2010**, *163*, 1091–1102. [CrossRef]

39. van den Besselaar, E.J.M.; Sanchez-Lorenzo, A.; Wild, M.; Klein Tank, A.M.G.; de Laat, A.T.J. Relationship between sunshine duration and temperature trends across Europe since the second half of the twentieth century. *J. Geophys. Res.* **2015**, *120*, 10823–10836. [CrossRef]

40. Macias-Fauria, M.; Johnson, E.A. Warming-induced upslope advance of subalpine forest is severely limited by geomorphic processes. *Proc. Natl. Acad. Sci. USA* **2013**, *110*, 8117–8122. [CrossRef]

41. Hagedorn, F.; Gavazov, K.; Alexander, J.M. Above- and belowground linkages shape responses of mountain vegetation to climate change. *Science* **2019**, *365*, 1119–1123. [CrossRef]

42. Brodersen, C.R.; Germino, M.J.; Johnson, D.M.; Reinhardt, K.; Smith, W.K.; Resler, L.M.; Bader, M.Y.; Sala, A.; Kueppers, L.M.; Broll, G.; et al. Seedling Survival at Timberline Is Critical to Conifer Mountain Forest Elevation and Extent. *Front. For. Glob. Chang.* **2019**, *2*, 9. [CrossRef]